Near Fermi level Electronic Structure of $Pr_{1-x}Sr_xMnO_3$: Photoemission Study

P. Pal, M. K. Dalai, R. Kundu, M. Chakraborty and B. R. Sekhar*
Institute of Physics, Sachivalaya Marg, Bhubaneswar 751 005, India.

C. Martin
Laboratoire CRISMAT, UMR 6508, ISMRA, Boulevard du Marechal Juin, 14050 Caen, France

In this study, we report the observation of a pseudogap associated with the insulator-metal transition in compositions of $Pr_{1-x}Sr_xMnO_3$ system with no charge ordering. Our valence band photoemission study shows that the observed shifts in the near Fermi level density of states are abrupt at the Curie transtion and occur over an energy scale of $\sim$ 1 eV, strongly suggesting that the charge-ordering gap observed earlier in other manganites and the pseudogap observed here may indeed have same origin. These results could be understood within the framework of models based on electronic phase separation where it has been shown that the pseudogap is a generic feature of the mixed-phase compositions. Also, our band structure calculations on $Pr_{0.75}Sr_{0.25}MnO_3$ show the possible existence of half-metallicity in this system.

PACS numbers: 79.60.-i, 75.47.Gk, 71.30.+h
Keywords: Photoemission spectroscopy, CMR, Insulator-metal transitions

I. INTRODUCTION

The near Fermi level electronic structure of colossal magnetoresistance (CMR) materials[1] ($RE_{1-x}AE_xMnO_3$, RE = rare earth, AE = alkaline earth) have been attracting much interest recently, particularly due to their importance in understanding the mechanism behind the insulator-metal (IM) transitions in these oxides. The ground state properties of these manganites are dominated mainly by the competition among four independent interactions: the magnetic interaction between the Mn e_g electron spins, the electron-phonon coupling, the electronic repulsion and the kinetic energy of the carriers. The behavior of doped manganites for $x < 0.5$ and $x > 0.5$ is drastically different and depends strongly on the competition among the above four interactions. These distorted perovskites undergo a transition from a ferromagnetic metallic (FMM) state to an antiferromagnetic insulating (AFMI) state with the doping of charge carriers. However, for a commensurate fraction of the carrier concentration, the FMM state is easily suppressed by the formation of different types of charge-ordering (CO). For example, CO in narrow one-electron bandwidth materials like $Pr_{0.5}Ca_{0.5}MnO_3$ and $La_{0.5}Ca_{0.5}MnO_3$ is charge-exchange (CE) type checkerboardlike. On the other hand, CO in wide one-electron bandwidth material like $Pr_{0.5}Sr_{0.5}MnO_3$ is "stripe-like"[2]. The FMM to CO insulating transition is caused by a spin and orbital-ordering of the carriers.

There have been several experimental investigations on the valence-band electronic structure of manganites[3,4,5]. Recent photoemission studies have highlighted the importance of the subtle changes in the density of states (DOS) at the Fermi level (E_F) in understanding the nature of the IM transitions of these manganites[6,7,8,9,10,11]. Many of the theoretical models, particularly those based on electronic phase separation also emphasize on the importance of these states[12,13,14]. Chainani *et al.*[6] have shown that some of the DOS very close to E_F get shifted to higher binding energies ($\sim$ 1.2 eV from E_F) and consequently a CO gap of $\sim$ 100 meV opens up at the transition. These authors have remarked that such spectral weight transfer could be a generic feature of CO gap in manganites. Similar studies on the CO compositions of $Pr_{1-x}Ca_xMnO_3$ are also reported[10,11]. Although, the mechanism of this CO gap is still not clear, the large energy scale over which the spectral weight get transferred shows the possibility of Coulombic origin. From the point of view of different theoretical models, it is quite likely that the pseudogap (PG) associated with the IM transitions, observed in double layered manganites by Saitoh it et al.[7] has the same origin as the CO gap. Such a generality in the shifts of near E_F DOS is interesting to be probed. Apart from the photoemission studies, PGs associated with the IM transitions of manganites were confirmed also using scanning tunneling spectroscopic studies[15,16].

In order to understand the nature of the near E_F spectral weight shifts in systems with no CO, we have studied some of the compositions of the $Pr_{1-x}Sr_xMnO_3$. The electrical and magnetic phase diagram of this system has been published earlier[17]. Different structural and magnetization studies[17,18,19,20] have shown that there exists no CO in any of the compositions in the $Pr_{1-x}Sr_xMnO_3$ system. However, a neutron diffraction study by Kajimoto *et al.*[2] showed that the $Pr_{0.5}Sr_{0.5}MnO_3$ sample had an anisotropic "stripe-like" CO. Below the Curie transition (T_C), this system is FMM for $0.25 < x < 0.5$, A-type AFMI for $0.5 < x < 0.7$ and C-type AFMI for $0.7 < x < 0.9$. For identifying the nature of the bands contributing to the near E_F DOS, we studied one of the relevant compositions of the $Pr_{1-x}Sr_xMnO_3$ system using the theoretical band structure calculation method based on local spin-density approximation incorporating the electron correlation (LSDA+U). The main part of this paper describes the results of our high resolution

photoelectron spectroscopic (PES) study of the near E_F states of some compositions of this system. Our studies show a shift in the near E_F spectral weight displaying a PG behavior. As per our knowledge, there has been no study reported earlier on the PG behavior of cubic manganites with no CO, using photoelectron spectroscopy.

II. EXPERIMENT AND CALCULATIONS

Polycrystalline samples of the $Pr_{1-x}Sr_xMnO_3$ system were prepared by solid state reactions[17]. Purity and cationic homogeneity of all the samples were systematically checked by electron diffraction coupled with energy dispersive spectroscopy analysis. Resistivity and magnetic behavior of the samples have been studied using the four probe technique and SQUID magnetometry. Details of the sample preparation, characterization and structural studies are published elsewhere along with a phase diagram[17,21,22].

Angle integrated ultraviolet photoemission measurements were performed using an Omicron mu-metal UHV system equipped with a high intensity vacuum-ultraviolet source (HIS 13) and a hemispherical electron energy analyzer (EA 125 HR). At the He I ($h\ \nu$ = 21.2 eV) line, the photon flux was of the order of 10^{16} photons/sec/steradian with a beam spot of 2.5 mm diameter. Fermi energies for all measurements were calibrated using a freshly evaporated Ag film on a sample holder. The total energy resolution, estimated from the width of the Fermi edge, was about 80 meV for He I excitation. All the photoemission measurements were performed inside the analysis chamber under a base vacuum of $\sim 1.0 \times 10^{-10}$ mbar. The polycrystalline samples were repeatedly scraped using a diamond file inside the preparation chamber with a base vacuum of $\sim 1.0 \times 10^{-10}$ mbar and the high-resolution spectra were taken within 1 hour to avoid surface degradation. The measurements were repeated to ensure reproducibility of the spectra. For the temperature dependent measurements, the samples were cooled by pumping liquid nitrogen through the sample manipulator fitted with a cryostat. Sample temperatures were measured using a silicon diode sensor touching the bottom of the stainless steel sample plate.

The LSDA+U band-structure calculations for $Pr_{0.75}Sr_{0.25}MnO_3$ were done for the ferromagnetic phase within the frame work of tight-binding Linear Muffin-Tin Orbitals (LMTO) method in the atomic sphere approximation[23,24]. Though, this composition has a slightly lower hole content (x) than the most important sample (x = 0.35) of the experimental part of this study, we have chosen it for the convenience of calculation. Nevertheless, both these compositions show similar electrical and magnetic properties as per the phase diagram of this system[17]. The crystal structure of $Pr_{0.75}Sr_{0.25}MnO_3$, we have used for the LSDA+U super-cell calculation is that of the parent compound $PrMnO_3$ (space group: Pbnm)[18]. The unit cell taken

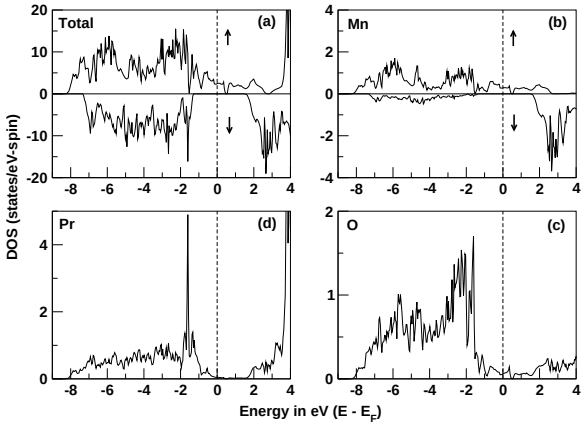

FIG. 1: Band structure of $Pr_{0.75}Sr_{0.25}MnO_3$ calculated using the LSDA + U method. (a) shows the total spin projected DOS. (b), (c) and (d) show the site projected DOS. The total spin projected DOS shows the half-metallic behavior of this composition.

was four formula unit. We have substituted one of the Pr atoms with a Sr atom. The exchange term J and the correlation term U for Pr $4f$ state are 0.95 eV and 7 eV respectively and that for Mn $3d$ is 0.87 eV and 4 eV respectively. The k-mesh used for the self-consistent calculation is (10×10×10).

III. RESULTS AND DISCUSSION

In Fig. 1 (a) we present the total DOS of $Pr_{0.75}Sr_{0.25}MnO_3$ calculated using the LSDA + U method. We have chosen this composition for a comparison with our experimental results and the issues addressed in this paper. The finite DOS near the E_F in Fig. 1(a) shows that $Pr_{0.75}Sr_{0.25}MnO_3$ is metallic, consistent with the phase diagram reported earlier[17]. The near E_F states are dominated by the Mn and O. From their individual DOS (Fig.1(b) and 1(c)) it is quite clear that there is a strong hybridization between the Mn $3d$ and the O $2p$ states through out the valence band. Though, the Pr $4f$ states appear at around 2 eV from the E_F, the electronic properties of this system are dominated by the Mn $3d$ states close to E_F. The states closest to the E_F are due to the Mn 3d e_g orbitals. As per our knowledge there has been no earlier reports published on the band structure calculations of this composition. However, the results of our calculation are in agreement with the LMTO and LSDA calculations reported earlier on similar systems[25,26]. Figs. 1(b), 1(c) and 1(d) show the site projected DOS for $Pr_{0.75}Sr_{0.25}MnO_3$. Based on the total spin projected DOS (Fig. 1(a)), we predict that $Pr_{0.75}Sr_{0.25}MnO_3$ could exhibit a half-metallic behavior, though there have been no experimental evi-

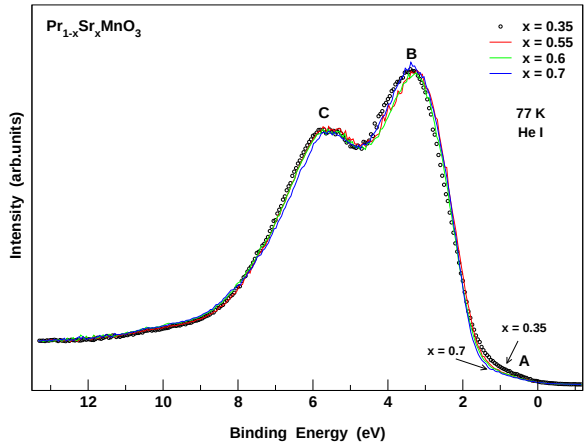

FIG. 2: (Color online) The experimental valence band photoemission spectra of the $Pr_{1-x}Sr_xMnO_3$ samples with $x = 0.35$, 0.55, 0.6 and 0.7 taken at 77 K ($h\nu = 21.2$ eV).

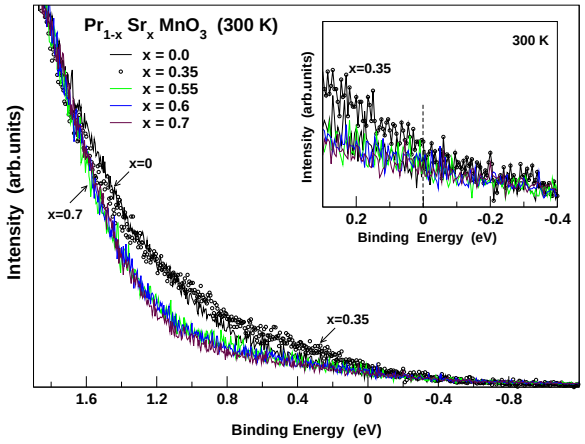

FIG. 3: (Color online) Doping dependent near E_F high-resolution photoemission spectra of $Pr_{1-x}Sr_xMnO_3$ compound taken at 300 K. All the spectra have been normalized to the integrated intensities in the energy region displayed here. The inset shows the spectral changes in the vicinity of E_F at 300 K.

dence to support this. The majority band is conducting whereas the minority band is clearly insulating; the hallmark of half-metallicity. The minority Mn band has very little population below E_F, consequently Mn atoms in $Pr_{0.75}Sr_{0.25}MnO_3$ has a substantially high magnetic moment. The calculated magnetic moment of individual Mn atom in $Pr_{0.75}Sr_{0.25}MnO_3$ is 3.88 μ_B. The total magnetic moment of the super-cell is 15 μ_B. The integral magnetic moment is the signature of the resulting half-metallicity. Half-metallicity in these compositions are important for the understanding of CMR phenomena as well as their technological applications in spintronics. A detailed study of the half-metallic compositions of this system is being published elsewhere[27].

Figure 2 shows the experimental valence band photoemission spectra of the $Pr_{1-x}Sr_xMnO_3$ samples with x = 0.35, 0.55, 0.6 and 0.7 taken at 77 K using UV photons of energy 21.2 eV. The spectra exhibit three features A (0.7 eV), B (3.3 eV) and C (5.5 eV) derived mainly from the hybridized Mn $3d$ - O $2p$ states in agreement with our calculations shown in Fig. 1. The feature A is due to Mn e_g spin-up states while the feature B has a strongly mixed character of Mn $3d$ t_{2g}, O $2p$ and Pr $4f$ states. The feature C has a dominant O $2p$ character with a small Mn $3d$ contribution. These assignments are consistent with the earlier reports on related manganites using photoemission spectroscopy[5,6,8,9,10,28]. Due to the large ionization cross-section, at this photon energy, the O $2p$ contribution to the spectra is high compared to the Pr $4f$ and Mn $3d$. As one can see from the figure, the intensity of feature (A) decreases systematically with increasing Sr content (x). The figure also shows that there are no drastic changes in the features B and C as a function of composition, which is again consistent with earlier experiments[3,4]. It is to be noted that the

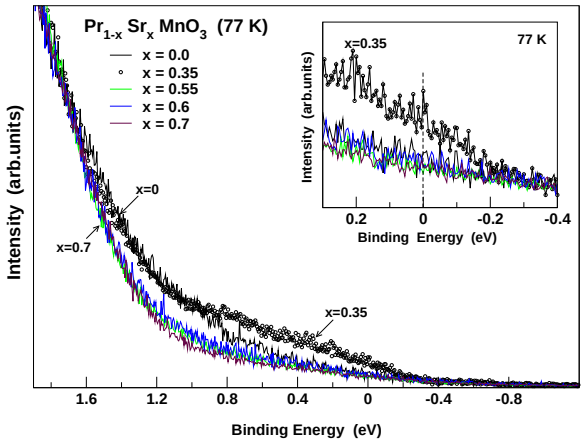

FIG. 4: (Color online) The near E_F photoemission spectra of $Pr_{1-x}Sr_xMnO_3$ compound taken at 77 K. The inset shows the spectral changes in the vicinity of E_F at 77 K.

$Pr_{0.65}Sr_{0.35}MnO_3$ sample has a significantly high spectral intensity near the E_F, depicting the metallic nature of this composition.

In this paper we concentrate on these near E_F electronic states responsible for most of the electrical and magnetic properties of $Pr_{1-x}Sr_xMnO_3$ system. In order to study these states, we have performed our temperature dependent high resolution PES measurements on the $Pr_{1-x}Sr_xMnO_3$ compounds. Figure 3 shows the near E_F spectra for various concentrations taken at 300 K. The spectra are normalized by the integrated intensity be-

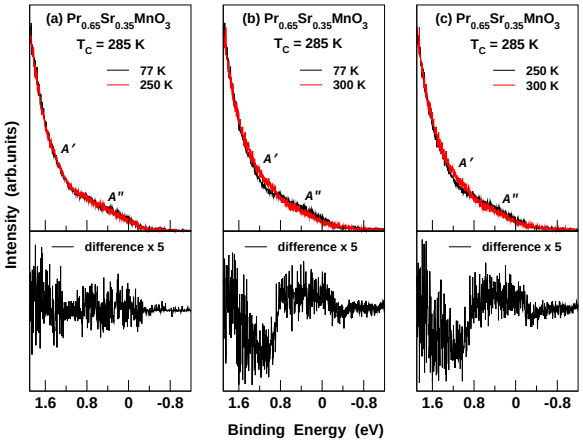

FIG. 5: (Color online) The near E_F high-resolution spectra of $Pr_{0.65}Sr_{0.35}MnO_3$ taken as a function of temperature (a) at T= 77 and 250 K, indicating negligible changes in the FMM phase with temperature, (b) at T= 77 and 300 K, and (c) at T= 250 and 300 K, across the FMM-PMI transition at $T_C = 285$ K showing a spectral weight transfer with decreasing temperature. Lower panels show the difference in spectra magnified by a factor of 5.

low E_F and all above 1.7 eV. One can see that the near E_F spectral weight gradually decreases as we go from the parent compound ($x = 0.0$) to $x = 0.7$, except in case of the $Pr_{0.65}Sr_{0.35}MnO_3$. Though, this systematic decrease is expected as the average e_g electron number decreases with increasing x, the $x = 0.35$ sample shows a comparatively high spectral weight near E_F, despite its insulating nature at this temperature. Figure 4 presents the high resolution PES spectra of all the samples taken at 77 K. At this temperature the $Pr_{0.65}Sr_{0.35}MnO_3$ sample shows FMM properties and all other compositions are insulating[17]. Again, these low temperature spectra show almost no change in the near E_F spectral weight compared to that taken at room temperature, except for the $x = 0.35$ which shows a distinct increase in these states. This increase indicates the metallic behavior of $Pr_{0.65}Sr_{0.35}MnO_3$ at 77 K. The insets of Fig. 3 (300 K) and Fig. 4 (77 K) provide a closer view of the intensity changes in a narrow energy region near E_F. A comparison of the two insets will further demonstrate that except the $x = 0.35$ all other samples show negligible change with lowering of temperature from 300 K to 77 K.

We have further analyzed this near E_F spectral weight change in case of the $Pr_{0.65}Sr_{0.35}MnO_3$ sample in order to understand its temperature dependence and origin. In Fig. 5 we compare the near E_F spectra obtained at 77 K (well below the paramagnetic insulating (PMI) to FMM transition, T_C), 250 K (below the T_C) and 300 K (above the T_C). The two spectra taken at 77 K and 250 K plotted together (Fig. 5(a)) show little change in their near E_F spectral weight as a function of temperature, whereas the 250 K and 300 K spectra (Fig. 5(c)) show a shift of spectral weight from the feature marked A" to A' as we go across the FMM-PMI transition. Such a shift is visible between the 77 K and 300 K spectra (Fig. 5(b)) also. Interestingly, the magnitude of the spectral weight shift between A" to A' remains the same for the 250 K or 77 K, showing that below T_C no further shift of spectral weight occurs with temperature. This shift of spectral weight from A" to A' while going across the FMM to PMI state shows the opening up of a gap at T_C. Since, the PMI state also shows a finite amount of states at the E_F, we prefer to call this a PG. From the difference spectra shown in the lower panels it is clear that this PG occurs due to the shift of states over an energy scale ~ 1.0 eV. In other words, ~ 1.0 eV (difference between A' and A") is required for the delocalization of the charge carriers to form the FMM state from the localized insulating state in this system. Now, looking back at Fig. 3 will reveal that the energy position of A' is the same as that of the spectral bump shown by the parent compound ($PrMnO_3$) at ~ 1.2 eV below E_F, which corresponds to the localized e_g states in this insulator. When the charge carrier concentration, x is increased to 0.35 these localized e_g states melt to the position of A" due to the changes in the overlap of Mn $3d$ - O $2p$ orbitals, as a consequence of the structural changes (Mn-O-Mn bond angles). This delocalization becomes stronger below T_C resulting in the metallic behavior of $x = 0.35$ sample.

As mentioned earlier, there have been a few studies using PES on the CO gap in similar systems[6,8,9,10,11]. Although, none of our $Pr_{1-x}Sr_xMnO_3$ samples show any CO at any temperature, the energy scale involved in the shift of states from A' to A" in our spectra is comparable to the value (1.2 eV) observed in a CO composition[6]. This indicates that the PG observed here and the CO gap are similar in nature, suggesting a common origin for both. As we have seen in the Fig. 5 the spectral weight shift in the $Pr_{0.65}Sr_{0.35}MnO_3$ sample from A' to A" across the T_C (300 K to 250 K) remains the same even with cooling down to 77 K. This shows there is no further temperature dependent delocalization of charge carriers except at the T_C. Again, this is another similarity between the CO gap and the PG, that both are abrupt at T_C with no temperature dependencies above or below[6]. These similarities may further suggest that a delocalization of the charge carriers and thereby a shift of the near E_F DOS is generic to the IM transitions in these manganites, regardless of the presence or absence of any CO.

The shift of electron states from near E_F to the energies above it, is an important result in understanding the CMR effect. Moreo *et al.* have shown that such PG can well be accounted in models based on electronic phase separation[13]. In these models, the PG behavior was found to be robust in systems with mixed-phase characteristics, where FMM clusters exist in an insulating background. The abrupt nature of the PG at T_C found in our study also can be understood, since these mixed

phase tendencies are strong at temperatures around T_C. Signatures of mixed phases are visible even at temperatures above or below the T_C, in the form of the absence of a sharp Fermi edge even in FMM phases and the existence of a finite number of states at the E_F in the PMI state. Monte Carlo calculations[12] predict that the PG at the chemical potential should be generic of mixed phases.

IV. CONCLUSION

Our studies using UV photoelectron spectroscopy show that the shifts of DOS near the E_F observed across the IM transitions in compositions of the $Pr_{1-x}Sr_xMnO_3$ system with no CO, are abrupt at the T_C and occur over an energy scale of ~ 1 eV. The energy scale involved in this PG formation and the abrupt nature of it near the T_C, strongly suggest that the CO gap observed earlier in other manganites and the PG may indeed have same origin. Further, we infer from our results as well as the results shown by Chainani *et al.*[6] and Saitoh *et al.*[7] that such shifts of the near E_F DOS could be generic to the IM transitions in the CMR compounds, regardless of the presence or absence of any charge ordering. The PG observed associated with the IM transition in $Pr_{0.65}Sr_{0.35}MnO_3$, shows the delocalization of the charge carriers involved. Our results could be understood within the framework of models based on the electronic phase separation where it has been shown that the PG is a common behavior of CMR compositions with mixed-phase character. Our theoretical band structure calculations using LSDA + U method on $Pr_{0.75}Sr_{0.25}MnO_3$, which is close in character to the $x = 0.35$ sample, show the possible existence of half-metallicity in this system.

* Electronic address: sekhar@iopb.res.in

[1] See Colossal magnetoresistive oxides, edited by Y. Tokura (Gordon and Breach science publishers, 2000).

[2] R. Kajimoto, H. Yoshizawa, Y. Tomioka, and Y. Tokura, Phys. Rev. B **66**, 180402(R) (2002).

[3] D. D. Sarma, N. Shanthi, S. R. Krishnakumar, T. Saitoh, T. Mizokawa, A. Sekiyama, K. Kobayashi, A. Fujimori, E. Weschke, R. Meier, G. Kaindl, Y. Takeda, and M. Takano, Phys. Rev. B **53**, 6873 (1996).

[4] J.-H. Park, C. T. Chen, S-W. Cheong, W. Bao, G. Meigs, V. Chakarian, and Y. U. Idzerda, Phys. Rev. Lett. **76**, 4215 (1996).

[5] M. K. Dalai, P. Pal, B. R. Sekhar, N. L. Saini, R. K. Singhal, K. B. Garg, B. Doyle, S. Nannarone, C. Martin, and F. Studer, Phys. Rev. B **74**, 165119 (2006) and references therein.

[6] A. Chainani, H. Kumigashira, T. Takahashi, Y. Tomioka, H. Kuwahara, and Y. Tokura, Phys. Rev. B **56**, R15513 (1997).

[7] T. Saitoh, D. S. Dessau, Y. Moritomo, T. Kimura, Y. Tokura, and N. Hamada, Phys. Rev. B **62**, 1039 (2000).

[8] A. Sekiyama, S. Suga, M. Fujikawa, S. Imada, T. Iwasaki, K. Matsuda, T. Matsushita, K. V. Kaznacheyev, A. Fujimori, H. Kuwahara, and Y. Tokura, Phys. Rev. B **59**, 15528 (1999).

[9] J.-S. Kang, C. G. Olson, J. H. Jung, S. T. Lee, T. W. Noh, and B. I. Min, Phys. Rev. B **60**, 13257 (1999).

[10] K. Ebata, H. Wadati, M. Takizawa, A. Fujimori, A. Chikamatsu, H. Kumigashira, M. Oshima, Y. Tomioka, and Y. Tokura, Phys. Rev. B **74**, 64419 (2006).

[11] K. Ebata, M. Hashimoto, K. Tanaka, A. Fujimori, Y. Tomioka, and Y. Tokura, Phys. Rev. B **76**, 174418 (2007).

[12] A. Moreo, S. Yunoki, and E. Dagotto, Phys. Rev. Lett. **83**, 2773 (1999).

[13] A. Moreo, S. Yunoki, and E. Dagotto, Science **283**, 34 (1999).

[14] H. Aliaga, D. Magnoux, A. Moreo, D. Poilblanc, S. Yunoki, and E. Dagotto, Phys. Rev. B **68**, 104405 (2003).

[15] J. Mitra, M. Paranjape, A. K. Raychaudhuri, N. D. Mathur, and M. G. Blamire, Phys. Rev. B **71**, 094426 (2005).

[16] J. Mitra, A. K. Raychaudhuri, Ya. M. Mukovskii, and D. Shulyatev, Phys. Rev. B **68**, 134428 (2003).

[17] C. Martin, A. Maignan, M. Hervieu, and B. Raveau, Phys. Rev. B **60**, 12191 (1999).

[18] Z. Jirak, S. Krupicka, Z. Simsa, M. Dlouha, and S. Vartislav, J. Magn. Magn. Mater. **53**, 153 (1985).

[19] K. Knizek, J. Hejtmanek, Z. Jirak, C. Martin, M. Hervieu, B. Raveau, G. Andre, and F. Bouree, Chem. Mater. **16**, 1104 (2004).

[20] H. Kawano, R. Kajimoto, H. Yoshizawa, Y. Tomioka, H. Kuwahara, and Y. Tokura, Phys. Rev. Lett. **78**, 4253 (1997).

[21] C. Martin, A. Maignan, M. Hervieu, B. Raveau, Z. Jirak, M. M. Savosta, A. Kurbakov, V. Trounov, G. Andre, and F. Bouree, Phys. Rev. B **62**, 6442 (2000).

[22] M. Hervieu, Chem. Mater **12**, 1456 (2000).

[23] V. I. Anisimov, J. Zaanen, and O. K. Andersen, Phys. Rev. B **44**, 943 (1991).

[24] V. I. Anisimov, F. Aryasetiawan, and A. I. Lichtenstein, J. Phys. Condens. Matter **9**, 767 (1997).

[25] W. E. Pickett, and D. J. Singh, Phys. Rev. B **53**, 1146 (1996).

[26] S. Satpathy, Z. S. Popovic, and F. R. Vukajlovic Phys. Rev. Lett. **76**, 960 (1996).

[27] M. Chakraborty, P. Pal, and B. R. Sekhar, Solid State Commun., **145**, 197 (2008).

[28] T. Saitoh, A. E. Bocquet, T. Mizokawa, H. Namatame, A. Fujimori, M. Abbate, Y. Takeda, and M. Takano, Phys. Rev. B **51**, 13942 (1995).